PHYSICAL REVIEW B VOLUME 26, NUMBER 5 1 SEPTEMBER 1982

Flux-line-cutting losses in type-II superconductors

John R. Clem
Ames Laboratory and Department of Physics, Iowa State University, Ames, Iowa 50011
(Received 23 November 1981; revised manuscript received 12 March 1982)

Energy dissipation associated with flux-line cutting (intersection and cross-joining of adjacent nonparallel vortices) is considered theoretically. The flux-line-cutting contribution to the dissipation per unit volume, arising from mutual annihilation of transverse magnetic flux, is identified as $\vec{J}_{\parallel}\cdot\vec{E}_{\parallel}$, where $\vec{J}_{\parallel}$ and $\vec{E}_{\parallel}$ are the components of the current density and the electric field parallel to the magnetic induction. The dynamical behavior of the magnetic structure at the flux-line-cutting threshold is shown to be governed by a special critical-state model similar to that proposed by previous authors. The resulting flux-line-cutting critical-state model, characterized in planar geometry by a parallel critical current density $J_{c\parallel}$ or a critical angle gradient k_c, is used to calculate predicted hysteretic ac flux-line-cutting losses in type-II superconductors in which the flux pinning is weak. The relation of the theory to previous experiments is discussed.

I. INTRODUCTION

The response of a vortex array subjected to a parallel transport current in a type-II superconductor is still not clearly understood. Recent experimental and theoretical investigations[1–43] indicate that, at a sufficiently high current density, instabilities occur which somehow produce a macroscopic electric field $\vec{E}$ with a component parallel to the macroscopic magnetic induction $\vec{B}$. This electric field is difficult to understand, because it is inconsistent with the expression[44,45] $\vec{E}=\vec{B}\times\vec{v}$, which is known to apply to flux flow with velocity $\vec{v}$ when the current density $\vec{J}$ is perpendicular to $\vec{B}$. Various authors have suggested[9–11,13,19,20,24,25,41,42] that a spatially inhomogeneous magnetic structure might explain why $\vec{E}$ can be parallel to $\vec{B}$ on the average, but so far there exists no theory capable of yielding quantitative predictions, e.g., for ac losses. Other authors have suggested[39,46] that flux-line cutting (intersection and cross-joining of adjacent nonparallel vortices) is responsible for the electric field. In this paper I shall explore the latter possibility and shall show how a macroscopic theory incorporating flux-line cutting can be formulated. In particular, I shall assume that flux-line cutting is the mechanism of primary physical importance to explain the most significant experimentally observed phenomena; I shall assume that spatial and temporal inhomogeneities,[11,19,24,25,38,40] although they ultimately will need to be accounted for to explain several sample-dependent effects, are mechanisms of secondary physical importance.

An important conclusion of this paper is that the dynamical behavior of vortex arrays at the flux-line-cutting threshold is naturally described by a special critical state model similar to that suggested by previous authors.[12,43,47–52] Various empirical critical state models characterized by a parallel critical current density[12,43] or a critical angle gradient[22,47–52] have been introduced previously, and several authors have mentioned the possible relationship of these models to flux-line cutting.[12,18,43,48,51] In this paper, however, I stress the intimacy of this relationship, and I show in detail how the parallel critical current density, the critical angle gradient, and the parallel component of the electric field are understood physically in terms of flux-line cutting.

In Sec. II I discuss energy dissipation, giving special attention to the flux-line-cutting contribution. I introduce in Sec. III a flux-line-cutting critical state model for planar geometry and apply it in Sec. IV to calculate ac flux-line-cutting losses. In Sec. V I summarize the most important results, relate the theory to previous experiments, and point out some unresolved questions.

II. ENERGY DISSIPATION

The rate of energy dissipation in a type-II superconductor is $\vec{J}\cdot\vec{E}$, where $\vec{J}=\vec{\nabla}\times\vec{H}$ is the macroscopic, coarse-grained current density, and $\vec{E}$ is the electric field. If the magnetic induction is written as $\vec{B}=B\hat{\alpha}$, the current density can be expressed as

$$\vec{J}=\vec{J}_{\parallel}+\vec{J}_{\perp}=J_{\parallel}\hat{\alpha}+J_{\perp}\hat{\beta}\ ,$$

where $\hat{\alpha}$ and $\hat{\beta}$ are unit vectors parallel and perpendicular to $\vec{B}$.

We identify $\vec{J}_\perp \cdot \vec{E}$ as the flux-flow contribution to the dissipation. When $\vec{J}_{||}=0$, the electric field can be written as[44,45] $\vec{E}=\vec{B}\times\vec{v}$, where $\vec{v}$ is the common flux-flow velocity of moving vortices. Then $\vec{J}_\perp \cdot \vec{E}=\vec{F}_L \cdot \vec{v}$ is the rate at which the Lorentz force per unit volume, $\vec{F}_L=\vec{J}\times\vec{B}$, does work on the vortex array. When $\vec{J}_{||}\neq 0$ and flux-line cutting occurs, however, we have[3,16,17] $\vec{E}=\vec{E}_{||}+\vec{E}_\perp$, where $\vec{E}_{||}$ is the component along $\vec{B}$ arising from flux-line cutting, and $\vec{E}_\perp=\vec{B}\times\vec{v}$ is the component perpendicular to $\vec{B}$ arising from flux flow. During flux-line cutting, the vortices do not all move locally with the same velocity but instead undergo complicated countermotion and intersection to generate $\vec{E}_{||}$.[3,16,17] With $\vec{v}$ defined as the average velocity of vortex line elements within a small volume V around the observation point $\vec{r}$, the expression $\vec{E}_\perp=\vec{B}\times\vec{v}$ remains valid and $\vec{J}_\perp \cdot \vec{E}_\perp=\vec{F}_L \cdot \vec{v}$ is still the rate at which the Lorentz force does work by moving the array as a whole.

We identify $\vec{J}_{||}\cdot\vec{E}_{||}$ as the flux-line-cutting contribution to the dissipation. Two conditions must be met for such dissipation to occur. First, the current density must have a component parallel to $\vec{B}$, and second, this component must be large enough to exceed the threshold for flux-line cutting.[18]

To go into further detail, let us use planar geometry. Consider a high-κ, type-II superconductor filling the half-space $x>0$. A time-dependent external magnetic induction $\vec{B}_s(t)=\mu_0\vec{H}_s(t)$, applied parallel to the surface, induces fields in the superconductor $\vec{B}$, $\vec{J}$, and $\vec{E}$, which are parallel to the yz plane and which depend only upon the coordinate x and the time t. We assume that B is sufficiently large ($B \gg \mu_0 H_{c1}$) that $B=\mu_0 H$ to good approximation. We further assume that the length scale for spatial variation of $\vec{B}$, $\vec{J}$, and $\vec{E}$ is much larger than the weak-field penetration depth λ. We express the magnetic induction as $\vec{B}=B\hat{\alpha}$, where $B=|\vec{B}|$ and

$$\hat{\alpha}=\hat{y}\sin\alpha+\hat{z}\cos\alpha \ . \tag{1}$$

With the definition

$$\hat{\beta}=\hat{\alpha}\times\hat{x}=\hat{y}\cos\alpha-\hat{z}\sin\alpha \ , \tag{2}$$

we obtain from Ampere's law, $\vec{J}=\vec{\nabla}\times\vec{H}$, the result $\vec{J}=J_{||}\hat{\alpha}+J_\perp\hat{\beta}$, where

$$J_{||}=\mu_0^{-1}B\frac{\partial\alpha}{\partial x} \ , \tag{3}$$

$$J_\perp=-\mu_0^{-1}\frac{\partial B}{\partial x} \ . \tag{4}$$

Faraday's law, $\vec{\nabla}\times\vec{E}=-\partial\vec{B}/\partial t$, yields

$$\frac{\partial\vec{E}}{\partial x}=\hat{\alpha}B\frac{\partial\alpha}{\partial t}-\hat{\beta}\frac{\partial B}{\partial t} \ . \tag{5}$$

Equation (5) must be supplemented with the condition, derived from fluxoid conservation, that $\vec{E}=0$ in any portion of the superconductor in which there is no vortex motion. We define the density of y and z flux quanta as $n_y=B_y/\phi_0$ and $n_z=B_z/\phi_0$, where $\phi_0=h/2e=2.07\times10^{-15}$ V s. By the Josephson condition[44,53] $2eV=h\nu$, we then can express

$$E_y=\phi_0\nu_z \ , \tag{6}$$

where ν_z is the net rate at which positive-z flux quanta (i.e., in the direction of $\hat{z}$) are carried in the positive-x direction (and/or negative-z flux quanta are carried in the negative-x direction) across unit length in the y direction.[16] Similarly,

$$E_z=-\phi_0\nu_y \ , \tag{7}$$

where ν_y is the net rate at which positive-y flux quanta (i.e., in the direction of $\hat{y}$) are carried in the positive-x direction (and/or negative-y flux quanta are carried in the negative-x direction) across unit length in the z direction.[16]

Expressions similar to (6) and (7) can be derived for the longitudinal and transverse components of the electric field, $\vec{E}=E_{||}\hat{\alpha}+E_\perp\hat{\beta}$. We have

$$E_\perp=\phi_0\nu_{||} \ , \tag{8}$$

where $\nu_{||}$ is the net rate at which longitudinal flux quanta (i.e., in the direction of $\hat{\alpha}$) are carried in the x direction across unit length in the transverse ($\hat{\beta}$) direction. Similarly,

$$E_{||}=-\phi_0\nu_\perp \ , \tag{9}$$

where $\nu_\perp$ is the net rate at which transverse flux quanta (i.e., in the direction of $\hat{\beta}$) are carried in the x direction across unit length in the longitudinal ($\hat{\alpha}$) direction. The longitudinal component $E_{||}$ is nonvanishing only when flux-line cutting occurs, i.e., when nonparallel vortices moving in opposite directions intersect. Briefly speaking, the transverse electric field is produced by transport of longitudinal flux and the longitudinal electric field by transport of transverse flux.

The flux-line cutting dissipation $\vec{J}_{||}\cdot\vec{E}_{||}=J_{||}E_{||}$ can be interpreted as arising from the mutual annihilation of transverse flux. Consider two adjacent slabs of magnetic flux in which $\vec{B}$ has the same magnitude but different directions before flux-line cutting. If the vortices in the slabs undergo flux-line cutting, the longitudinal flux (in the direction of the average $\vec{B}$) is conserved, but the transverse flux density of the two slabs is mutually annihilated. Flux-line cutting thus dissipates the field energy initially associated with the transverse components of the magnetic flux.

To demonstrate this, let the two slabs each be of thickness $\Delta x/2$ and lie on either side of the plane $x=x_0$. In the slab centered on $x=x_0\pm\Delta x/4$, the initial magnetic induction is

$$\vec{B}=B_0[\pm\hat{y}\sin(\Delta\alpha/2)+\hat{z}\cos(\Delta\alpha/2)] ,$$

where $\Delta\alpha \ll 1$. Before flux-line cutting, the field energy density in the region $|x-x_0|<\Delta x/2$ is $B_0^2/2\mu_0$. During flux-line cutting, the vortices from the region $x_0<x<x_0+\Delta x/2$ intersect the vortices from the region $x_0-\Delta x/2<x<x_0$, and the transverse (y-directed) magnetic flux is mutually annihilated. Because the longitudinal flux is conserved, the final magnetic induction is $B_0\hat{z}\cos(\Delta\alpha/2)$, and the final field energy density in the region $|x-x_0|<\Delta x/2$ is $(B_0^2/2\mu_0)\cos^2(\Delta\alpha/2)$. The average energy per unit volume dissipated in the region $|x-x_0|<\Delta x/2$ is the difference between the final and initial field energies,

$$W_v=B_0^2(\Delta\alpha)^2/8\mu_0 . \tag{10}$$

(Recall that $\Delta\alpha \ll 1$.)

The average parallel current density in the region $|x-x_0|<\Delta x/2$ is, from (3),

$$J_z=B_0\Delta\alpha/\mu_0\Delta x . \tag{11}$$

A positive-z component of the electric field arises because during flux-line cutting positive-y flux quanta move in the negative-x direction and negative-y flux quanta move in the positive-x direction. The time integral of E_z over the flux-line cutting process is, from (7),

$$\int dt\, E_z=B_0\sin(\Delta\alpha/2)(\Delta x/2-|x-x_0|) . \tag{12}$$

Averaged over the region $|x-x_0|<\Delta x/2$, this yields ($\Delta\alpha \ll 1$)

$$\int dt\, \bar{E}_z=B_0\Delta\alpha\Delta x/8 . \tag{13}$$

Combining (11) and (13), we obtain the total dissipation averaged over the thickness Δx,

$$\int dt\, J_z\bar{E}_z=B_0^2(\Delta\alpha)^2/8\mu_0 , \tag{14}$$

in agreement with (10).

The above discussion of flux-line-cutting dissipation employs only macroscopic electrodynamics. A deeper understanding of this dissipation would require microscopic electrodynamics. Here one would consider time-dependent deformations of a vortex array, the complicated trajectories of individual vortex line elements, and the local balance of driving and viscous forces on these line elements. The rate of dissipation per unit length of a line element dl of vortex i moving with velocity $\vec{v}_i(l,t)$ is[45,54] $\eta v_i^2(l,t)$, where η is the viscous drag coefficient per unit length. If all the $\vec{v}_i(l,t)$ were known, the macroscopic rate of dissipation per unit volume at $\vec{r}$ and t, corresponding to $\vec{J}_{||}\cdot\vec{E}_{||}$, could be calculated by integrating $\eta v_i^2(l,t)$ over the lengths of all vortices contained within a small volume V centered at $\vec{r}$ and dividing the result by V.

III. FLUX-LINE-CUTTING CRITICAL STATE MODEL

Consider a nearly reversible, high-κ, semi-infinite type-II superconductor in the space $x>0$, which has been cooled in field in an applied magnetic induction $B_0\hat{z}$ ($\mu_0H_{c1} \ll B_0<\mu_0H_{c2}$). Suppose now that the applied magnetic induction in the space $x<0$ is rotated through an angle α_s but held fixed in magnitude, such that at the surface ($x=0$) the final magnetic induction is $\vec{B}_s=B_0\hat{\alpha}_s$, where

$$\hat{\alpha}_s=\hat{y}\sin\alpha_s+\hat{z}\cos\alpha_s . \tag{15}$$

What is the resulting distribution of $\vec{B}$ and $\vec{J}$ in the superconductor?

The Lorentz force per unit volume in the x direction is $F_{Lx}=J_\perp B$, where $J_\perp$ is given by (4). In the presence of pinning, the usual critical state model requires that F_{Lx} be balanced by a pinning force density $F_p=J_{c\perp}B$, such that $|J_\perp|=J_{c\perp}(B,T)$, where $J_{c\perp}$ is the transverse critical current density. Here, however, we consider a superconductor in which flux pinning is very weak. Thus, in equilibrium the flux distribution inside the superconductor must be essentially force-free: $F_{Lx}\approx 0$, $J_\perp\approx 0$, and from (4) $B=|\vec{B}|\approx B_0$.

We next address the question of how $\vec{B}(x)=B_0\hat{\alpha}(x)$ varies with x. We assume that $\vec{B}(0)=\vec{B}_s$ and $\hat{\alpha}(0)=\hat{\alpha}_s$, i.e., that the surface cannot carry a surface current. We also assume that deep within the superconductor $\vec{B}=B_0\hat{z}$. How then does the field angle $\alpha(x)$ vary from its value α_s at the surface to its value 0 deep inside? Note from (3) that wherever α varies with x,

$$J_{||}(x)=\mu_0^{-1}B_0\frac{\partial\alpha(x)}{\partial x} . \tag{16}$$

By analogy with the flux-pinning critical state model, there is a characteristic *parallel critical current density* $J_{c||}(B,T)$, which cannot be exceeded in metastable equilibrium. There is also a corresponding *critical angle gradient* $k_c(B,T)$, defined via (16) or

$$k_c(B,T)=\mu_0 J_{c\|}(B,T)/B \ , \tag{17}$$

which cannot be exceeded in metastable equilibrium. In this model, flux configurations produced in the superconductor are governed by the equivalent equations

$$J_{\|}(x)=\pm J_{c\|}(B,T) \ , \tag{18}$$

$$\frac{\partial \alpha(x)}{\partial x}=\pm k_c(B,T) \ , \tag{19}$$

the upper or lower signs being chosen according to the particular history of $\vec{B}_s(t)=B_0\hat{\alpha}_s(t)$. Vortex configurations described by (18) and (19) are at the *flux-line-cutting threshold.*[18] Current densities and angle gradients whose magnitudes are in excess of $J_{c\|}$ and k_c produce flux-line cutting, an electric field, and magnetic flux redistribution.

The dynamical behavior of vortices at the flux-line-cutting threshold thus is naturally described in terms of Eqs. (18) and (19), which can be regarded as a special critical state model for a vortex array subjected to parallel supercurrents. Previous authors have introduced similar empirical critical state models with quantities analogous to the parallel critical current density[12,43] or the critical angle gradient,[22,47–52] and have used such models to understand a considerable amount of experimental data.

A number of theoretical calculations that relate to $J_{c\|}$ have been carried out. An upper limit to $J_{c\|}$ for $T\simeq T_c$ and $B\approx B_{c2}=\mu_0 H_{c2}$ is provided by the Ginzburg-Landau theory for the depairing critical current density flowing parallel to a rigid lattice of straight vortices[55] or to locally parallel helical vortices with equal pitch,[56]

$$J_{\text{dep}}=0.470(H_c/\lambda)(1-b)^{3/2}/(1-\tfrac{1}{2}\kappa^2) \ , \tag{20}$$

where H_c is the bulk thermodynamic critical field and $b=B/B_{c2}$. In Ref. 57 it is argued that essentially the same expression holds for $T\approx 0$ K. It is also shown in Ref. 57 that in the limit as $b\to 0$ the depairing current density remains proportional to H_c/λ, with the constant of proportionality given by 0.60 as $T\to 0$ K and 0.54 as $T\to T_c$. It is shown in Ref. 15, however, that a single straight vortex subjected to a sufficiently large parallel applied current density is unstable: If the applied current density points, for example, in the same direction as the vortex's magnetic field, a left-handed helical distortion of the vortex becomes unstable and grows in amplitude. The resulting increase in line energy is more than compensated by the energy gained from the source of the applied current, and the overall Gibbs free energy is reduced. The longitudinal critical current density at the onset of the helical expansion instability recently has been calculated from the London theory for an array of *parallel* vortices near the surface or in the bulk, including the influence of flux pinning.[2,4–7] All the expressions for the longitudinal critical current density apparently yield values less than the depairing critical current density.

A numerical calculation of $J_{c\|}$ vs b was presented in Ref. 18 for an array of *nonparallel* vortices undergoing a different kind of instability. For several reasons, however, this calculation again provides only an upper limit to $J_{c\|}$: Some other kind of instability, such as the helical expansion instability,[15] may break up the vortex structure and lead to flux-line cutting at values of $J_{c\|}$ well below those found for the instability considered in Ref. 18. Moreover, it was assumed in Ref. 18 that all vortices remain straight at the onset of the instability. Recent calculations[58] have revealed that bending of vortices at crossover points greatly reduces the repulsive forces between adjacent nonparallel vortices. This indicates that calculations allowing for vortex bending would produce much smaller values of $J_{c\|}$ than in Ref. 18. Finally, inclusion of depairing effects, not considered in Ref. 18, also would yield smaller values of $J_{c\|}$.

Thus, despite the existing calculations, the longitudinal critical current density $J_{c\|}$ at the flux-line-cutting threshold is not well determined theoretically. Neither the dependences upon B and T nor the numerical values of $J_{c\|}$ are known beyond question. The calculations of Refs. 5–7 and 18, however, do suggest that, for $b \ll 1$, $J_{c\|}$ is a monotonically *increasing,* sometimes even linear, function of $b=B/B_{c2}$ but that, as $b\to 1$, $J_{c\|}$ vanishes as some still unknown power n of $(1-b)$. If $J_{c\|}$ approaches J_{dep} as $b\to 1$, the exponent n ultimately cannot exceed $\frac{3}{2}$, if Eq. (20) is to be satisfied. The B dependence thus is not expected to be the same as that of the transverse, depinning critical current density $J_{c\perp}$, which normally is a monotonically *decreasing* function of B. Indeed, the results of Boyer *et al.*,[48] when reinterpreted in terms of $J_{c\|}$ and $J_{c\perp}$, indicate that at $T=4.2$ K the field dependences of $J_{c\|}$ and $J_{c\perp}$ for the V and VTi samples they studied are related to good approximation via $J_{c\|}=kBJ_{c\perp}$, where k is a material-dependent constant. In the absence of a well-established general theory for $J_{c\|}$ valid for arbitrary materials, however, it is appropriate to regard $J_{c||}(B,T)$ as an experimentally measurable quantity, as is usually done for the case of the flux-pinning critical current density $J_{c\perp}(B,T)$.

IV. AC FLUX-LINE-CUTTING LOSSES

In this section we use the critical state model of Sec. III to calculate the ac losses near the surface of a nearly reversible, high-κ, semi-infinite type-II superconductor in the region $x>0$. To focus on flux-line-cutting losses, we assume that the specimen has a negligible amount of bulk pinning and essentially no surface barrier to vortex entry or exit. The losses arise in response to a time-varying external magnetic induction applied parallel to the surface, $\vec{B}_s(t)=B_0\hat{\alpha}_s(t)$ [see Eq. (15)]. The field angle $\alpha_s(t)$ sweeps periodically back and forth between the values $-\alpha_0$ and $+\alpha_0$, where $\alpha_0<\pi$. At the end of this section we discuss the predicted behavior when $\alpha_0>\pi$. We assume that the sweep rate is sufficiently slow that eddy-current losses are negligible. The losses are then entirely hysteretic, and the dissipated energy per cycle is independent of the frequency. Moreover, provided α_s varies monotonically between the extremal values $\pm\alpha_0$, the loss per cycle is independent of the waveform of $\alpha_s(t)$; e.g., sinusoidal, triangular, or trapezoidal waveforms all yield the same loss per cycle.

To calculate the flux-line-cutting losses, our method is to: (a) determine the field angle profiles $\alpha(x,t)$ vs x using the critical state model of Sec. III, (b) obtain $\vec{B}(x,t)=B_0\hat{\alpha}(x,t)$ using Eq. (1), (c) find $\vec{E}(0,t)$ with the help of Faraday's law, and (d) calculate the losses using Poynting's theorem. In several respects, our approach parallels the calculation for pinning losses, as outlined in Ref. 59.

The required field angle profiles [$\alpha(x,t)$ vs x] are sketched in Fig. 1. The two extremal profiles, $\alpha_{\max}(x)$ and $\alpha_{\min}(x)$, correspond to the cases when $\alpha_s=\alpha_0$ and $\alpha_s=-\alpha_0$, respectively. From Eq. (19) we obtain for $0\le x\le x_c$,

$$\alpha_{\max}(x)=\alpha_0-k_cx \ , \tag{21}$$

$$\alpha_{\min}(x)=-\alpha_0+k_cx \ . \tag{22}$$

The maximum depth of penetration of the critical state profiles is

$$x_c=\alpha_0 k_c \ . \tag{23}$$

For $x>x_c$, $\alpha(x,t)=0$.

Starting from the profile $\alpha_{\min}(x)$ when $\alpha_s=-\alpha_0$, we consider the profile $\alpha_\uparrow(x,t)$ as α_s increases.[60] The altered portion of the profile for $0\le x\le x_\uparrow(t)$ is

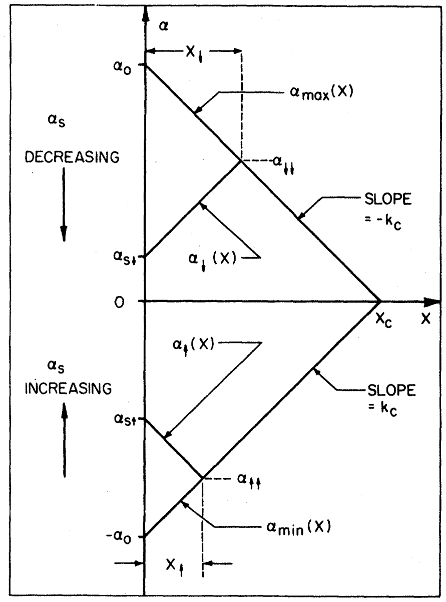

FIG. 1. Sketch of the extremal field angle profiles, $\alpha_{\max}$ and $\alpha_{\min}$, and the α_s-increasing and α_s-decreasing profiles, $\alpha_\uparrow$ and $\alpha_\downarrow$, vs x, calculated from the flux-line-cutting critical state model, $\partial\alpha/\partial x=\pm k_c$. Here, $\alpha_0<\pi$.

$$\alpha_\uparrow(x,t)=\alpha_s(t)-k_cx \ , \tag{24}$$

where

$$x_\uparrow(t)=\frac{\alpha_0+\alpha_s(t)}{2k_c} \ . \tag{25}$$

For $x_\uparrow(t)\le x\le x_c$, $\alpha_\uparrow(x,t)=\alpha_{\min}(x)$. At $x=x_\uparrow(t)$,

$$\alpha_\uparrow(x_\uparrow,t)=\alpha_{\uparrow\uparrow}(t)=\frac{\alpha_s(t)-\alpha_0}{2} \ . \tag{26}$$

Similarly, the profile $\alpha_\downarrow(x,t)$ for the α_s-decreasing case is given in the region $0\le x\le x_\downarrow(t)$ by

$$\alpha_\downarrow(x,t)=\alpha_s(t)+k_cx \ , \tag{27}$$

where

$$x_\downarrow(t)=\frac{\alpha_0-\alpha_s(t)}{2k_c} \ . \tag{28}$$

For $x_\downarrow(t)\le x\le x_c$, $\alpha_\downarrow(x,t)=\alpha_{\max}(x)$. At $x=x_\downarrow(t)$,

$$\alpha_\downarrow(x_\downarrow,t)=\alpha_{\downarrow\downarrow}(t)=\frac{\alpha_s(t)+\alpha_0}{2} \ . \tag{29}$$

Consider now the fields $\vec{E}_\uparrow(x,t)$ and $\vec{B}_\uparrow(x,t)$ for the α_s-increasing case.[60] From (5) we obtain

$$\left[\frac{\partial}{\partial x}\right]\vec{E}_\uparrow(x,t)=\dot{\alpha}_s\vec{B}_\uparrow(x,t) \ , \tag{30}$$

where $\dot{\alpha}_s=d\alpha_s/dt$. Note that by Eqs. (6)–(9)

$\vec{E}_\uparrow(x,t)=0$ for $x \geq x_\uparrow(t)$, because there is no flux motion or flux-line cutting in this region at time t. Thus, integration of (30) from $x=0$ to $x=x_\uparrow(t)$, where $\vec{E}_\uparrow=0$, yields

$$\vec{E}_\uparrow(0,t)=-\dot{\alpha}_s B_0 \int_0^{x_\uparrow(t)} dx[\hat{y}\sin\alpha_\uparrow(x,t) + \hat{z}\cos\alpha_\uparrow(x,t)] \; . \tag{31}$$

Changing variables from x to α, we obtain with the help of (24) and (26),

$$\vec{E}_\uparrow(0,t)=\left[\frac{\dot{\alpha}_s B_0}{k_c}\right][\hat{y}(\cos\alpha_s-\cos\alpha_{\uparrow\uparrow}) - \hat{z}(\sin\alpha_s-\sin\alpha_{\uparrow\uparrow})] \; . \tag{32}$$

Because $|\vec{B}_\uparrow(x,t)|=B_0$, Poynting's theorem[61] here states that the rate at which energy is dissipated per unit area is equal to the rate at which the source of the externally applied field does work per unit area of the specimen:

$$S_{\uparrow x}(0,t)=\hat{x}\cdot\vec{E}_\uparrow(0,t)\times\vec{B}_s(t)/\mu_0 = \frac{B_0^2\dot{\alpha}_s}{\mu_0 k_c}\left[1-\cos\left[\frac{\alpha_0+\alpha_s}{2}\right]\right] \; . \tag{33}$$

Integrating this over half a period, we obtain the energy dissipated per unit area during the α_s-increasing half-cycle,

$$W'_{a\uparrow}=\frac{2B_0^2}{\mu_0 k_c}(\alpha_0-\sin\alpha_0) \; . \tag{34}$$

Calculations similar to those leading to Eqs. (30)–(34) yield, for the rate of energy dissipation per unit area for α_s decreasing,

$$S_{\downarrow x}(0,t)=-\frac{B_0^2\dot{\alpha}_s}{\mu_0 k_c}\left[1-\cos\left[\frac{\alpha_0-\alpha_s}{2}\right]\right] \; . \tag{35}$$

The total energy dissipated per unit area during the α_s-decreasing half-cycle is the same as (34), such that the total flux-line-cutting energy loss per unit area per cycle is

$$W'_a=\frac{4B_0^3}{\mu_0^2 J_{c\parallel}(B_0,T)}(\alpha_0-\sin\alpha_0) \; . \tag{36}$$

For $\alpha_0 \ll 1$, we obtain to good approximation

$$W'_a=\frac{2b_{0\perp}^3}{3\mu_0^2 J_{c\parallel}(B_0,T)} \; , \tag{37}$$

where $b_{0\perp}=B_0\sin\alpha_0 \approx B_0\alpha_0$ is the maximum *transverse* component of the oscillating magnetic induction at the surface. Equation (37) bears a remarkable resemblance to

$$W'_{bp}=\frac{2b_{0\parallel}^3}{3\mu_0^2 J_{c\perp}(B_0,T)} \; , \tag{38}$$

the flux-pinning critical state result (bulk pinning, no surface barrier, and $B_0 \gg \mu_0 H_{c1}$) in a parallel applied dc magnetic induction $\vec{B}_0$ and an applied ac magnetic induction of amplitude $b_{0\parallel}$ *parallel* to $\vec{B}_0$.[59] In nearly reversible superconductors, however, we expect that $J_{c\perp} \ll J_{c\parallel}$, such that for the same ac amplitude b_0, the flux-line-cutting losses given in (37) should be much smaller than the flux-pinning losses given in (38).

Recent experiments by Boyer *et al.*,[48] on strong-pinning V and VTi specimens have been interpreted in terms of a critical state model similar to that of Eqs. (17)–(19). The analysis[48] reveals that, although $J_{c\parallel}$ and $J_{c\perp}$ have different B dependences, $J_{c\parallel}$ is about an order of magnitude larger than $J_{c\perp}$ over most of the magnetic field region investigated. If indeed the condition $J_{c\parallel} \gg J_{c\perp}$ is obeyed for nearly all fields in both weak-pinning and strong-pinning type-II superconductors, one can easily understand why the losses generated in response to an ac magnetic field of amplitude $\Delta H_\perp$ parallel to the surface can be reduced by an order of magnitude or more by applying a sufficiently large magnetic field $H_\parallel$ also parallel to the surface but perpendicular to the ac field.[22,49–51,62–67] The explanation is simply that in the absence of $H_\parallel$ the losses are the usual flux-pinning losses, characterized by $J_{c\perp}$ as in Eq. (38). When a sufficiently large $H_\parallel$ is applied, however, the net field applied at the surface remains close in magnitude to $H_\parallel$ but varies its angle with amplitude $\alpha_0=\Delta H_\perp/H_\parallel \ll 1$. For such conditions the dominant losses are flux-line-cutting losses, characterized by $J_{c\parallel}$ as in Eq. (37). When $J_{c\parallel} \gg J_{c\perp}$, the resulting flux-line-cutting losses are thus much less than the flux-pinning losses.

Let us now examine in more detail the electric field $\vec{E}_\uparrow(x,t)$ generated during the α_s-increasing half-cycle. By a method similar to that leading to (32), we obtain for $x \leq x_\uparrow(t)$,

$$\vec{E}_\uparrow(x,t)=(\dot{\alpha}_s B_0/k_c)\{\hat{y}[\cos\alpha_\uparrow(x,t)-\cos\alpha_{\uparrow\uparrow}(t)]-\hat{z}[\sin\alpha_\uparrow(x,t)-\sin\alpha_{\uparrow\uparrow}(t)]\} \; . \tag{39}$$

Both $E_{\uparrow y}$ and $E_{\uparrow z}$ vanish at $x=x_\uparrow$, where $\alpha_\uparrow(x_\uparrow)=\alpha_{\uparrow\uparrow}$. (See Fig. 1.) The longitudinal and transverse components of $\vec{E}_\uparrow$ are, for $x \leq x_\uparrow(t)$,

$$E_{\uparrow\parallel}(x,t)=\vec{E}_\uparrow(x,t)\cdot\hat{\alpha}_\uparrow(x,t)=-(\dot{\alpha}_s B_0/k_c)\sin[\alpha_\uparrow(x,t)-\alpha_{\uparrow\uparrow}(t)] , \quad (40)$$

$$E_{\uparrow\perp}(x,t)=\vec{E}_\uparrow(x,t)\cdot\hat{\beta}_\uparrow(x,t)=(\dot{\alpha}_s B_0/k_c)\{1-\cos[\alpha_\uparrow(x,t)-\alpha_{\uparrow\uparrow}(t)]\} . \quad (41)$$

Here

$$\hat{\alpha}_\uparrow(x,t)=\hat{y}\sin\alpha_\uparrow(x,t)+\hat{z}\cos\alpha_\uparrow(x,t) , \quad (42)$$

$$\hat{\beta}_\uparrow(x,t)=\hat{y}\cos\alpha_\uparrow(x,t)-\hat{z}\sin\alpha_\uparrow(x,t) \quad (43)$$

are the unit vectors parallel and perpendicular to $\vec{B}_\uparrow(x,t)$. Note that both $E_{\uparrow\parallel}$ and $E_{\uparrow\perp}$ vanish at $x=x_\uparrow$.

During the α_s-increasing half-cycle, the rate of energy dissipation per unit volume in the region $0\le x\le x_\uparrow(t)$ is $\vec{J}_\uparrow\cdot\vec{E}_\uparrow$. However, because $J_{\uparrow\perp}=0$, we have $\vec{J}_\uparrow=J_{\uparrow\parallel}\hat{\alpha}_\uparrow$, where, from (3), $J_{\uparrow\parallel}=-\mu_0^{-1}B_0k_c$. The transverse component of $\vec{E}_\uparrow$, i.e., $E_{\uparrow\perp}$, therefore does not contribute to the dissipation. The rate of energy dissipation per unit volume is then

$$J_{\uparrow\parallel}E_{\uparrow\parallel}(x,t)=\left[\frac{\dot{\alpha}_s B_0^2}{\mu_0}\right]\sin[\alpha_\uparrow(x,t)-\alpha_{\uparrow\uparrow}(t)] . \quad (44)$$

The integral of (44) from $x=0$ to $x=x_\uparrow(t)$ is $S_x(0,t)$, given by (33).

From Eqs. (6)–(9) and (39)–(41) we obtain the net rates at which flux quanta are transported in the x direction by flux-line-cutting processes. During the α_s-increasing half-cycle, we obtain for $0\le x\le x_\uparrow(t)$,

$$v_{\uparrow z}(x,t)=\left[\frac{\dot{\alpha}_s n_0}{k_c}\right][\cos\alpha_\uparrow(x,t)-\cos\alpha_{\uparrow\uparrow}(t)] , \quad (45)$$

$$v_{\uparrow y}(x,t)=\left[\frac{\dot{\alpha}_s n_0}{k_c}\right][\sin\alpha_\uparrow(x,t)-\sin\alpha_{\uparrow\uparrow}(t)] , \quad (46)$$

$$v_{\uparrow\parallel}(x,t)=\left[\frac{\dot{\alpha}_s n_0}{k_c}\right]\{1-\cos[\alpha_\uparrow(x,t)-\alpha_{\uparrow\uparrow}(t)]\} , \quad (47)$$

$$v_{\uparrow\perp}(x,t)=\left[\frac{\dot{\alpha}_s n_0}{k_c}\right]\sin[\alpha_\uparrow(x,t)-\alpha_{\uparrow\uparrow}(t)] , \quad (48)$$

where $n_0=B_0/\phi_0$. All these rates are zero for $x\ge x_\uparrow(t)$. The time integrals of $v_{\uparrow z}(x,t)$ and $v_{\uparrow y}(x,t)$ over the α_s-increasing half-cycle are, for $0\le x\le x_c$,

$$\Delta N'_{\uparrow z}(x)=\int dt\, v_{\uparrow z}(x,t)=0 , \quad (49)$$

$$\Delta N'_{\uparrow y}(x)=\int dt\, v_{\uparrow y}(x,t)=\left[\frac{2n_0}{k_c}\right][1-\cos\alpha_{\max}(x)] . \quad (50)$$

The above results provide a specific example of the more general phenomenon that *flux-line cutting consumes B*. For slab geometry in which $\vec{B}(x,t)=B(x,t)\hat{\alpha}(x,t)$, Faraday's law and Eqs. (1)–(4) can be used to derive

$$\frac{\partial B}{\partial t}+\left[\frac{\partial}{\partial x}\right]j_{Bx}=-\frac{\mu_0 J_\parallel E_\parallel}{B} , \quad (51)$$

where

$$j_{Bx}=Bv_x=E_\perp \quad (52)$$

is the B-current density. In the absence of flux-line cutting, $E_\parallel$, and thus the right-hand side of Eq. (51), vanish. The resulting equation is a continuity equation describing conservation of B: A local increase of B within a volume increment of the superconductor occurs only via the divergence of $\vec{j}_B$, i.e., via net transport of B in through the walls of the volume increment. On the other hand, in the presence of flux-line cutting, for which the corresponding dissipation is $J_\parallel E_\parallel>0$, the right-hand side of Eq. (51) is negative, indicating that a region of space in which flux-line cutting is occurring serves as a sink for B.

In experiments with slowly rotating disks of type-II superconductors,[47,48,68] rotation has been found to lower the value of B inside the superconductor. This phenomenon was interpreted as evidence that vortices could somehow be expelled from the specimen *against* an inwardly directed Lorentz force.[47,48,68] Flux-line cutting, on the other hand, provides a more natural explanation: Rotation induces flux-line cutting, which in turn lowers the local value of B. During continuous rotation, a steady state can be reached, in which $\partial B/\partial t=0$ and the local rate of decrease of B via flux-line cutting is exactly compensated by flux transport in the same direction as the Lorentz force.

Returning to the situation considered in this paper, we again have a case in which the local consumption of B via flux-line cutting is balanced via flux transport. Here $B(x,t)=B_0$, such that $\partial B/\partial t=0$. During the α_s-increasing half-cycle, for example, Eq. (51) yields

$$\left[\frac{\partial}{\partial x}\right]E_{\uparrow\perp}(x,t)=-\frac{\mu_0 J_{\uparrow\parallel}E_{\uparrow\parallel}(x,t)}{B_0}, \tag{53}$$

which easily can be verified using Eqs. (40) and (41) and $J_{\uparrow\parallel}=-B_0k_c/\mu_0$.

So far the above discussion has been restricted to angle amplitudes α_0 obeying $\alpha_0<\pi$. When $\alpha_0>\pi$, our flux-line-cutting model predicts a diverging energy dissipation for a semi-infinite superconductor as $J_{c\perp}\to 0$. The physics of this phenomenon can be understood by considering the behavior as α_s is slowly increased from zero, starting from an initial angle distribution $\alpha(x,0)=0$. The profiles of $\alpha(x,t)$ are then as sketched in Fig. 2. When $\alpha_s<\pi$, we have $\alpha(x,t)=\alpha_s-k_cx$ in the region $0\le x\le\alpha_s/k_c$, as in Fig. 2(a). A calculation similar to that leading to Eq. (40) yields

$$E_{\parallel}(x,t)=-\left[\frac{\dot{\alpha}_sB_0}{k_c}\right]\sin\alpha(x,t)\,. \tag{54}$$

Because $J_{\parallel}=-J_{c\parallel}=-B_0k_c/\mu_0$, the corresponding dissipation $J_{\parallel}E_{\parallel}$ is positive in the region $0\le x<\alpha_s/k_c$ when $\alpha_s<\pi$. When $\alpha_s=\pi$, however, $J_{\parallel}E_{\parallel}$ becomes equal to zero at the surface, and $\alpha(x,t)$ is as sketched in Fig. 2(b). Equation (54) cannot remain valid for $\alpha_s>\pi$, because it would yield positive values of $E_{\parallel}$ and negative values of the dissipation $J_{\parallel}E_{\parallel}$.

Instead, for α_s slightly greater than π, time-dependent profiles of $\alpha(x,t)$ as sketched in Figs. 2(c) and 2(d) must occur. For Fig. 2(c), for example, $\alpha=0$ for $x\ge x_1$, $\alpha=k_c(x_1-x)$ for $x_2\le x\le x_1$, and $\alpha\approx\pi$ for $x\le x_2$, where $k_c(x_1-x_2)=\pi$. Flux-line cutting occurs only within the zone $x_2<x<x_1$, where

$$E_{\parallel}(x,t)=-B_0\dot{x}_1\sin\alpha(x,t)\,, \tag{55}$$

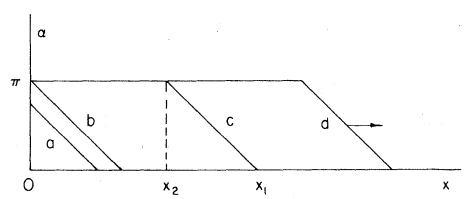

FIG. 2. Sketch of profiles of $\alpha(x,t)$ vs x predicted by the flux-line-cutting model when $J_{c\perp}=0$ for various values of $\alpha_s=\alpha(0,t)$: (a) $\alpha_s<\pi$, (b) $\alpha_s=\pi$, (c) and (d) $\alpha_s\gtrsim\pi$, for which the flux-line-cutting zone ($x_2<x<x_1$) moves spontaneously and irreversibly into the specimen (arrow).

$$E_{\perp}(x,t)=B_0\dot{x}_1[1-\cos\alpha(x,t)]\,, \tag{56}$$

and $\dot{x}_1=dx_1/dt$. In the zone $0\le x\le x_2$ there occurs only flux transport and no flux-line cutting, such that $E_{\perp}=2B_0\dot{x}_1$ and $E_{\parallel}=0$. The flux-line-cutting zone moves spontaneously and irreversibly into the specimen's interior. Behind this advancing zone, vortices with angle $\alpha\approx\pi$ are transported in the x direction with speed $v=2\dot{x}_1$, twice that of the zone. These vortices move into the flux-line-cutting zone, where they are consumed. The net effect of the zone motion is to annihilate vortices with $\alpha=0$ and to replace them with vortices with $\alpha=\pi$. The rate at which the source of the applied magnetic field does work per unit surface area of the superconductor is $S_{\perp}=E_{\perp}B_0/\mu_0=2B_0{}^2\dot{x}_1/\mu_0$. For nonvanishing $J_{c\perp}$, the zone penetrates only to a depth $x_1\sim x_0=B_0/\mu_0J_{c\perp}$. The energy loss per unit surface area that occurs during the spontaneous penetration of the flux-line-cutting zone is thus of order $B_0^3/\mu_0^2J_{c\perp}$, which diverges as $J_{c\perp}\to 0$. Further details of this effect and related phenomena will be described in a subsequent publication.

V. SUMMARY AND DISCUSSION

The theory of the electrodynamic properties of type-II superconductors in longitudinal geometry, where $\vec{J}$ has a component parallel to $\vec{B}$, is in a primitive state by comparison with the theory for transverse geometry, where $\vec{J}$ is always perpendicular to $\vec{B}$. Although flux-line cutting has been suspected to play an important role in the longitudinal case, it so far has not been incorporated into a complete electrodynamic theory of type-II superconductors. In this paper I have attempted to explore some of the consequences of flux-line cutting and to construct at least a partial quantitative theory with some predictive power. As discussed in the previous sections, flux-line cutting leads to the following behavior:

(a) Flux-line cutting generates a component, $\vec{E}_{\parallel}$, of the electric field *parallel* to the macroscopic magnetic induction $\vec{B}$.

(b) This longitudinal electric field component is produced by net transport of *transverse* flux quanta, such transport being accomplished by the intersection of locally countermoving vortices.

(c) The total rate $\vec{J}\cdot\vec{E}$ of dissipation per unit volume has *two* contributions: $\vec{J}_{\perp}\cdot\vec{E}_{\perp}$, which arises from flux flow and is already well understood in transverse geometry, and $\vec{J}_{\parallel}\cdot\vec{E}_{\parallel}$, which arises from flux-line cutting.

(d) The flux-line-cutting contribution $\vec{J}_{||}\cdot\vec{E}_{||}$ can be interpreted at the macroscopic level as arising from the mutual annihilation of transverse magnetic flux. At the microscopic level, this contribution comes from viscous losses, as vortex line segments locally execute complicated flux-line-cutting trajectories.

(e) Flux-line cutting implies *nonconservation of* B. A region of space in which flux-line cutting is occurring serves as a sink for B.

(f) A *flux-line-cutting critical state model,* parametrized by a parallel ($\vec{J}\,||\,\vec{B}$) critical current density $J_{c||}(B,T)$, as suggested by previous authors,[12,43,47–52] can be constructed. There are strong mathematical similarities to the flux-pinning critical state model, which is parametrized by a perpendicular ($\vec{J}\perp\vec{B}$) critical current density $J_{c\perp}(B,T)$.

(g) The flux-line-cutting critical state model easily can be applied to calculate the ac losses in nearly reversible type-II superconductors when only flux-line cutting produces dissipation. The result is given by Eq. (36).

Cave *et al.*[12] used an ac technique to measure magnetic flux penetration into a nearly reversible type-II superconducting wire (Pb−54 at. % In) in a parallel applied field. They observed hysteretic waveforms similar to those of the flux-pinning critical state model. The measured flux penetration, though completely inconsistent with the motion of unbroken helical vortices, could be understood qualitatively in terms of flux-line-cutting processes.[12] Interpretation of the results of Ref. 12 in terms of the flux-line-cutting critical state model of Sec. III yields a parallel critical current density $J_{c||}$ of order 10^3 A/cm^2, which is at least an order of magnitude larger than the measured transverse critical current density. Although all the results of Ref. 12 appear to be understandable in terms of a flux-line-cutting critical state model, the theory needs to be extended to cylindrical geometry before a detailed comparison can be made.

In the desired extension of the present theory to cylindrical and more complex geometry, it is likely that the concept of a parallel critical current density $J_{c||}$ (at the threshold of flux-line cutting) will remain useful. On the other hand, the equations governing the spatial variation of B and the field angle α will be somewhat more complex than Eqs. (3) and (4). Preliminary work suggests that at the critical dc current for the onset of the flux-line-cutting electric field, the longitudinal and azimuthal components of the magnetic induction in a nearly reversible type-II superconducting cylinder are well described by the familiar Bessel function solutions,[1]

$$B_z(\rho)=B_z(0)J_0(k_c\rho)\ , \tag{57}$$

$$B_\phi(\rho)=B_z(0)J_1(k_c\rho)\ , \tag{58}$$

but with the parameter k_c determined by $J_{c||}$ via $k_c=\mu_0 J_{c||}/B$. Here, ρ is the radial coordinate. Equations (57) and (58) should hold to good approximation provided B and $k_c(B)$ are nearly constant over the entire cross section, i.e., provided $k_c a<1$, where a is the specimen radius. Application of these results to Walmsley's experiments[39] on a Pb−40 at. % Tl alloy yields $J_{c||}$ typically of order 10^3 A/cm^2.

An extension of the theoretical framework of this paper to superconductors subject to flux pinning also is desirable, because this is the area in which most of the experimental data exists. In this case a combined flux-line-cutting and flux-pinning critical state model can be constructed, in which for planar geometry the spatial variation of α is governed by (3) with $|J_{||}|=J_{c||}$ and the spatial variation of B is governed by (4) with $|J_\perp|=J_{c\perp}$. The sign of $J_\perp$ must be chosen such that the volume pinning force $\vec{F}_p$, which balances the Lorentz force $\vec{F}_L=\vec{J}\times\vec{B}$ (i.e., $\vec{F}_p=-\vec{F}_L$), is oppositely directed to the average vortex line element velocity,

$$\vec{v}=\vec{E}_\perp\times\vec{B}/B^2=\mu_0\vec{S}/B^2\ .$$

It will be shown in a subsequent publication that inclusion of flux pinning as suggested above leads, for example, to the expression

$$W_a'=\frac{2b_{0\perp}^3}{3\mu_0^2 J_{c||}(B_0,T)}\left[1-\frac{J_{c\perp}(B_0,T)}{2J_{c||}(B_0,T)}\frac{b_{0\perp}}{B_0}\right] \tag{59}$$

for the energy loss per cycle per unit area corresponding to Eq. (37), provided $b_{0\perp}\ll B_0$ and $b_{0\perp}\le(J_{c||}/J_{c\perp})B_0$. The second term inside the large parentheses then represents only a small correction to Eq. (37), especially when $J_{c||}$ is an order of magnitude or so larger than $J_{c\perp}$.

An important unresolved question is the extent to which flux-line cutting and flux pinning influence each other: Does flux pinning increase or decrease $J_{c||}$? One can argue either that pinning locally stabilizes the vortex lattice,[5–7] such that $J_{c||}$ is increased, or that pinning sites facilitate flux-line cutting, such that $J_{c||}$ is decreased.[1,37,39,46] Similarly, does flux-line cutting increase or decrease $J_{c\perp}$? Here one might argue that, because adjacent vortices move in opposite directions during flux-line cutting, the sense of directionality of the pinning force is largely destroyed, such that $J_{c\perp}$ is reduced. Recent experiments,[48] however, suggest that $J_{c\perp}$ is essentially unaffected by flux-line cutting.

Also deserving theoretical attention are the spatial and temporal fluctuations in the longitudinal electric field observed during flux flow in current-carrying type-II superconductors subjected to parallel magnetic fields.[11,19,24,25,38,40] Whether these fluctuations result from sample inhomogeneities and are of secondary physical importance, as assumed here, or whether they result from essential magnetic structure inhomogeneities and are thus of primary physical importance, remains an open question.

ACKNOWLEDGMENTS

I am grateful to Dr. M. A. R. LeBlanc, Dr. R. Gauthier, Dr. A. Lachaine, Dr. F. Irie, Dr. K. Yamafuji, Dr. D. G. Walmsley, and Dr. E. H. Brandt for stimulating discussions and correspondence. I also thank Mr. Antonio Perez-Gonzalez for assistance in carrying out some numerical computations. Ames Laboratory is operated for the U.S. Department of Energy by Iowa State University under Contract No. W-7405-Eng-82. This work was supported by the Director for Energy Research, Office of Basic Energy Sciences.

---

[1]An excellent review of the literature as of 1974 regarding type-II superconductors subjected to parallel currents and fields is given by W. E. Timms and D. G. Walmsley, J. Phys. F 5, 287 (1975).

[2]E. H. Brandt, Phys. Lett. 79A, 207 (1980).

[3]E. H. Brandt, J. Low Temp. Phys. 39, 41 (1980).

[4]E. H. Brandt, J. Low Temp. Phys. 42, 557 (1981).

[5]E. H. Brandt, J. Low Temp. Phys. 44, 33 (1981).

[6]E. H. Brandt, J. Low Temp. Phys. 44, 59 (1981).

[7]E. H. Brandt, Physica 107B, 459 (1981).

[8]E. H. Brandt, J. R. Clem, and D. G. Walmsley, J. Low Temp. Phys. 37, 43 (1979).

[9]A. M. Campbell, Helv. Phys. Acta 53, 404 (1980).

[10]J. R. Cave, Ph.D. thesis, University of Cambridge, 1978 (unpublished).

[11]J. R. Cave and J. E. Evetts, Philos. Mag. B 37, 111 (1978).

[12]J. R. Cave, J. E. Evetts, and A. M. Campbell, J. Phys. (Paris) 39, C6-614 (1978).

[13]J. R. Clem, Phys. Lett. 54A, 452 (1975).

[14]J. R. Clem, Phys. Lett. 59A, 401 (1976).

[15]J. R. Clem, Phys. Rev. Lett. 38, 1425 (1977).

[16]J. R. Clem, J. Low Temp. Phys. 38, 353 (1980).

[17]J. R. Clem, Physica 107B, 453 (1981).

[18]J. R. Clem and S. Yeh, J. Low Temp. Phys. 39, 173 (1980).

[19]T. Ezaki and F. Irie, J. Phys. Soc. Jpn. 40, 382 (1976).

[20]T. Ezaki, K. Yamafuji, and F. Irie, J. Phys. Soc. Jpn. 40, 1271 (1976).

[21]G. Fillion, R. Gauthier, and M. A. R. LeBlanc, Phys. Rev. Lett. 43, 86 (1979).

[22]R. Gauthier, Ph.D. thesis, University of Ottawa, 1976 (unpublished).

[23]R. Gauthier, M. A. R. LeBlanc, and B. C. Belanger, in *Low Temperature Physics—LT13,* edited by K. D. Timmerhaus, W. J. O'Sullivan, and E. F. Hammel (Plenum, New York, 1974), Vol. 3, p. 241.

[24]F. Irie, T. Ezaki, and K. Yamafuji, in *International Discussion Meeting on Flux Pinning in Superconductors,* edited by H. C. Freyhardt (Akademie der Wissenschaften, Gottingen, 1975), p. 294.

[25]F. Irie, T. Ezaki, and K. Yamafuji, IEEE Trans. Magn. MAG-11, 332 (1975).

[26]V. G. Kogan, Phys. Rev. B 21, 2799 (1980).

[27]V. G. Kogan, Phys. Rev. B 21, 3027 (1980).

[28]V. G. Kogan, Phys. Lett. 79A, 337 (1980).

[29]Y. Kubota, T. Ogasawara, and K. Yasukochi, in *Proceedings of the 5th International Cryogenic Engineering Conference,* edited by K. Mendelssohn (IPC Science and Technology Press, Guildford, 1974), p. 135.

[30]J. R. Lorrain, M. A. R. LeBlanc, and A. Lachaine, Can. J. Phys. 57, 1458 (1979).

[31]B. Makiej, A. Sikora, S. Golab, and W. Zacharko, in *International Discussion Meeting on Flux Pinning in Superconductors,* edited by H. C. Freyhardt (Akademie der Wissenschaften, Gottingen, 1975), p. 305.

[32]B. Makiej, A. Sikora, G. Trojnar, S. Golab, and W. Zacharko, Cryogenics 16, 537 (1976).

[33]B. Makiej, S. Golab, A. Sikora, F. Trojnar, and W. Zacharko, in *Low Temperature Physics—LT14,* edited by M. Krusius and M. Vuorio (North-Holland, Amsterdam, 1975), Vol. 2, p. 141.

[34]J. F. Nicholson and P. T. Sikora, J. Low Temp. Phys. 17, 275 (1974).

[35]J. E. Nicholson, P. T. Sikora, and K. J. Carroll, in *Low Temperature Physics—LT13,* edited by K. D. Timmerhaus, W. J. O'Sullivan, and E. F. Hammel (Plenum, New York, 1974), p. 192.

[36]M. Sugahara, J. Phys. Soc. Jpn. 39, 1454 (1975).

[37]W. E. Timms and D. G. Walmsley, Phys. Status Solidi B 71, 741 (1975).

[38]W. E. Timms and D. G. Walmsley, J. Phys. F 6, 2107 (1976).

[39]D. G. Walmsley, J. Phys. F 2, 510 (1973).

[40]D. G. Walmsley and W. E. Timms, J. Phys. F 7, 2373 (1977).

[41]K. Yamafuji, in *International Discussion Meeting on Flux Pinning in Superconductors,* edited by H. C. Freyhardt (Akademie der Wissenschaften, Gottingen,

1975), p. 291.
[42]K. Yamafuji, T. Kawashima, and H. Ichikawa, J. Phys. Soc. Jpn. 39, 581 (1975).
[43]K. Yamafuji and T. Matsushita, J. Phys. Soc. Jpn. 47, 1069 (1979).
[44]B. D. Josephson, Phys. Lett. 16, 242 (1965).
[45]Y. B. Kim and M. J. Stephen, in *Superconductivity*, edited by R. D. Parks (Dekker, New York, 1969), Vol. 2, p. 1133.
[46]A. M. Campbell and J. E. Evetts, Adv. Phys. 21, 199 (1972).
[47]R. Boyer, Ph.D. thesis, University of Ottawa, 1977 (unpublished).
[48]R. Boyer, G. Fillion, and M. A. R. LeBlanc, J. Appl. Phys. 51, 1692 (1980).
[49]R. Gauthier and M. A. R. LeBlanc, IEEE Trans. Magn. MAG-13, 560 (1977).
[50]A. Lachaine, Ph.D. thesis, University of Ottawa, 1976 (unpublished).
[51]A. Lachaine, M. A. R. LeBlanc, and J. P. Lorrain, Physica 107B, 433 (1981).
[52]W. E. Timms, Phys. Lett. 40A, 427 (1972).
[53]B. D. Josephson, Adv. Phys. 14, 419 (1965).
[54]J. Bardeen and M. J. Stephen, Phys. Rev. 140, A1197 (1965).
[55]R. G. Boyd, Phys. Rev. 145, 255 (1966).
[56]F. F. Ternovskii, Zh. Eksp. Teor. Fiz. 60, 1790 (1971) [Sov. Phys.—JETP 33, 969 (1971)].
[57]R. D. Zaitsev, Zh. Eksp. Teor. Fiz. 61, 1620 (1971) [Sov. Phys.—JETP 34, 864 (1972)].
[58]P. Wagenleithner, Ph.D. thesis, University of Linz, 1981 (unpublished).
[59]J. R. Clem, J. Appl. Phys. 50, 3518 (1979).
[60]The subscripts ↑ and ↓ refer to the α_s-increasing and α_s-decreasing half-cycles, respectively.
[61]J. D. Jackson, *Classical Electrodynamics* (Wiley, New York, 1962), p. 189.
[62]A. Lachaine and M. A. R. LeBlanc, IEEE Trans. Magn. MAG-11, 336 (1975).
[63]Y. Nakayama, in *Proceedings of the 4th International Cryogenic Engineering Conference,* edited by K. Mendelssohn (IPC Science and Technology Press, Guildford, 1972), p. 133.
[64]Y. Nakayama, Y. Koike, and T. Toyoda, in *Proceedings of the 5th International Cryogenic Engineering Conference,* edited by K. Mendelssohn (IPC Science and Technology Press, Guildford, 1974), p. 129.
[65]M. Sugahara and S. Kato, Appl. Phys. Lett. 19, 111 (1971).
[66]M. Sugahara and N. Yamada, Jpn. J. Appl. Phys. 9, 1531 (1970).
[67]H. F. Taylor, Appl. Phys. Lett. 11, 169 (1967).
[68]R. Boyer and M. A. R. LeBlanc, Solid State Commun. 24, 261 (1977).